Publ. Astron. Soc. Japan (2016) 68 (6), 107 (1–14)
doi: 10.1093/pasj/psw101
Advance Access Publication Date: 2016 October 27

RZ Leonis Minoris bridging between ER Ursae Majoris-type dwarf nova and nova-like system

Taichi Kato,[1,*] Ryoko Ishioka,[2] Keisuke Isogai,[1] Mariko Kimura,[1] Akira Imada,[3] Ian Miller,[4] Kazunari Masumoto,[5] Hirochika Nishino,[5] Naoto Kojiguchi,[5] Miho Kawabata,[5] Daisuke Sakai,[5] Yuki Sugiura,[5] Hisami Furukawa,[5] Kenta Yamamura,[5] Hiroshi Kobayashi,[5] Katsura Matsumoto,[5] Shiang-Yu Wang,[2] Yi Chou,[6] Chow-Choong Ngeow,[6] Wen-Ping Chen,[6] Neelam Panwar,[6] Chi-Sheng Lin,[6] Hsiang-Yao Hsiao,[6] Jhen-Kuei Guo,[6] Chien-Cheng Lin,[6] Chingis Omarov,[7] Anatoly Kusakin,[7] Maxim Krugov,[7] Donn R. Starkey,[8] Elena P. Pavlenko,[9] Kirill A. Antonyuk,[9] Aleksei A. Sosnjvskij,[9] Oksana I. Antonyuk,[9] Nikolai V. Pit,[9] Alex V. Baklanov,[9] Julia V. Babina,[9] Hiroshi Itoh,[10] Stefano Padovan,[11] Hidehiko Akazawa,[12] Stella Kafka,[11] Enrique de Miguel,[13,14] Roger D. Pickard,[15,16] Seiichiro Kiyota,[17] Sergey Yu. Shugarov,[18,19] Drahomir Chochol,[19] Viktoriia Krushevska,[20] Matej Sekeráš,[19] Olga Pikalova,[21] Richard Sabo,[22] Pavol A. Dubovsky,[23] Igor Kudzej,[23] Joseph Ulowetz,[24] Shawn Dvorak,[25] Geoff Stone,[11] Tamás Tordai,[26] Franky Dubois,[27] Ludwig Logie,[27] Steve Rau,[27] Siegfried Vanaverbeke,[27] Tonny Vanmunster,[28] Arto Oksanen,[29] Yutaka Maeda,[30] Kiyoshi Kasai,[31] Natalia Katysheva,[18] Etienne Morelle,[32] Vitaly V. Neustroev,[33,34] and George Sjoberg[11,35]

[1]Department of Astronomy, Kyoto University, Kitashirakawa-Oiwake-cho, Sakyo-ku, Kyoto, Kyoto 606-8502, Japan
[2]Institute of Astronomy and Astrophysics, Academia Sinica, 11F of Astronomy-Mathematics Building, National Taiwan University, No. 1, Sec. 4, Roosevelt Rd, Taipei 10617, Taiwan
[3]Kwasan and Hida Observatories, Kyoto University, 17 Ohmine-cho Kita Kazan, Yamashina-ku, Kyoto, Kyoto 607-8471, Japan
[4]Furzehill House, Ilston, Swansea, SA2 7LE, UK
[5]Osaka Kyoiku University, 4-698-1 Asahigaoka, Kashiwara, Osaka 582-8582, Japan
[6]Graduate Institute of Astronomy, National Central University, Jhongli 32001, Taiwan
[7]Fessenkov Astrophysical Institute, Observatory 23, Almaty 050020, Kazakhstan
[8]DeKalb Observatory, H63, 2507 County Road 60, Auburn, IN 46706, USA
[9]Federal State Budget Scientific Institution "Crimean Astrophysical Observatory of RAS", Nauchny 298409, Republic of Crimea
[10]Variable Star Observers League in Japan (VSOLJ), 1001-105 Nishiterakata, Hachioji, Tokyo 192-0153, Japan
[11]American Association of Variable Star Observers, 49 Bay State Rd., Cambridge, MA 02138, USA

[12]Department of Biosphere-Geosphere System Science, Faculty of Informatics, Okayama University of Science, 1-1 Ridai-cho, Okayama, Okayama 700-0005, Japan
[13]Departamento de Ciencias Integradas, Facultad de Ciencias Experimentales, Universidad de Huelva, 21071 Huelva, Spain
[14]Center for Backyard Astrophysics, Observatorio del CIECEM, Parque Dunar, Matalascañas, 21760 Almonte, Huelva, Spain
[15]The British Astronomical Association, Variable Star Section (BAA VSS), Burlington House, Piccadilly, London, W1J 0DU, UK
[16]3 The Birches, Shobdon, Leominster, Herefordshire, HR6 9NG, UK
[17]VSOLJ, 7-1 Kitahatsutomi, Kamagaya, Chiba 273-0126, Japan
[18]Sternberg Astronomical Institute, Lomonosov Moscow State University, Universitetsky Ave., 13, Moscow 119992, Russia
[19]Astronomical Institute of the Slovak Academy of Sciences, 05960 Tatranska Lomnica, Slovakia
[20]Main Astronomical Observatory of the National Academy of Sciences of Ukraine, 27 Akademika Zabolotnoho ave., 03680 Kyiv, Ukraine
[21]Faculty of Physics, Lomonosov Moscow State University, Leninskie Gory, Moscow 119991, Russia
[22]2336 Trailcrest Dr., Bozeman, MT 59718, USA
[23]Vihorlat Observatory, Mierova 4, 06601 Humenne, Slovakia
[24]Center for Backyard Astrophysics Illinois, Northbrook Meadow Observatory, 855 Fair Ln, Northbrook, IL 60062, USA
[25]Rolling Hills Observatory, 1643 Nightfall Drive, Clermont, FL 34711, USA
[26]Polaris Observatory, Hungarian Astronomical Association, Laborc utca 2/c, 1037 Budapest, Hungary
[27]Public Observatory Astrolab Iris, Verbrandemolenstraat 5, B 8901 Zillebeke, Belgium
[28]Center for Backyard Astrophysics Belgium, Walhostraat 1A, B-3401 Landen, Belgium
[29]Hankasalmi Observatory, Vertaalantie 116, FIN-40500 Hankasalmi, Finland
[30]Kaminishiyamamachi 12-14, Nagasaki, Nagasaki 850-0006, Japan
[31]Baselstrasse 133D, CH-4132 Muttenz, Switzerland
[32]9 rue Vasco de GAMA, 59553 Lauwin Planque, France
[33]Finnish Centre for Astronomy with ESO (FINCA), University of Turku, Väisäläntie 20, FIN-21500 Piikkiö, Finland
[34]Astronomy Research Unit, PO Box 3000, FIN-90014 University of Oulu, Finland
[35]The George-Elma Observatory, 9 Contentment Crest, #182, Mayhill, NM 88339, USA

*E-mail: tkato@kusastro.kyoto-u.ac.jp

Received 2016 September 5; Accepted 2016 September 20

Abstract

We observed RZ LMi, which is renowned for its extremely short (∼19 d) supercycle and is a member of a small, unusual class of cataclysmic variables called ER UMa-type dwarf novae, in 2013 and 2016. In 2016, the supercycles of this object substantially lengthened in comparison to the previous measurements to 35, 32, and 60 d for three consecutive superoutbursts. We consider that the object virtually experienced a transition to the nova-like state (permanent superhumper). This observed behavior reproduced the prediction of the thermal-tidal instability model extremely well. We detected a precursor in the 2016 superoutburst and detected growing (stage A) superhumps with a mean period of 0.0602(1) d in 2016 and in 2013. Combined with the period of superhumps immediately after the superoutburst, the mass ratio is not as small as in WZ Sge-type dwarf novae, having orbital periods similar to RZ LMi. By using least absolute shrinkage and selection operator (Lasso) two-dimensional power spectra, we detected possible negative superhumps with a period of 0.05710(1) d. We estimated an orbital period of 0.05792 d, which suggests a mass ratio of 0.105(5). This relatively large mass ratio is even above that of

ordinary SU UMa-type dwarf novae, and it is also possible that the exceptionally high mass-transfer rate in RZ LMi may be a result of a stripped secondary with an evolved core in a system evolving toward an AM CVn-type object.

Key words: accretion, accretion disks — novae, cataclysmic variables — stars: dwarf novae — stars: individual (RZ Leonis Minoris)

1 Introduction

SU UMa-type dwarf novae (DNe) are a class of cataclysmic variables (CVs) which are close binary systems transferring matter from a red dwarf secondary to a white dwarf, forming an accretion disk. In SU UMa-type DNe, two types of outbursts are seen: normal outbursts and superoutbursts. Superoutbursts are defined by the presence of (positive) superhumps, which are humps with a period that is a few percent longer than the orbital period [for general information on CVs, DNe, SU UMa-type DNe, and superhumps, see e.g., Warner (1995)].

RZ LMi is one of the most enigmatic SU UMa-type DNe. This object was originally discovered as an ultraviolet-excess variable star [Lipovetskii & Stepanyan 1981; it was later given a designation of FBS 0948+344 (Abrahamian & Mickaelian 1993)]. Lipovetskii and Stepanyan (1981) reported that the object had a spectral energy distribution of spectral classes O–B at maximum. When the object was fading or rising, strong emission lines appeared. Lipovetskii and Stepanyan (1981) studied 16 objective prism plates and seven direct imaging plates and recorded a strong variation with a range of 14–17 mag. The object was recorded at 17 mag on the Palomar Obervatory Sky Survey (POSS). Based on the colors and rapid variation in a time-scale of a few days, Lipovetskii and Stepanyan (1981) suggested a dwarf nova-type classification. Green et al. (1982) also selected it as an ultraviolet-excess object (PG 0948+344) and confirmed it spectroscopically as a CV. They gave a variability range of $B = 14.4$–16.8 without details (the minimum likely referred to the magnitude in POSS). Despite the finding by Lipovetskii and Stepanyan (1981), Kholopov et al. (1985) designated RZ LMi as a nova-like (NL) variable by referring to Green et al. (1982). Kondo, Noguchi, and Maehara (1984) also selected RZ LMi as an ultraviolet-excess object.

The nature of the variability of this object remained unclear. Knowing the dwarf nova-type classification, one of the authors of this paper (TK) visually observed this object in 1987–1988 and found relatively stable ~20 d cycle lengths with additional short outbursts. This result was reported in the domestic variable star bulletin "Henkousei" (in Japanese). This report was probably the first to document the unusual cyclic variation of RZ LMi. Two teams observed this object photometrically: Robertson, Honeycutt, and Turner (1994) reported an unusual long-term repetitive light curve with a stable period (it is now known as the supercycle) of 19.2 d. Pikalova and Shugarov (1995) reported that the behavior was different from a typical dwarf nova in that it showed short fading and brightening. They also reported a possible period of 21.167 d or 23.313 d, and classified it as a VY Scl-type NL.

A clue to understanding the unusual behavior of RZ LMi came from the discovery of the SU UMa-type dwarf nova ER UMa with an ultrashort supercycle (interval between superoutbursts) of 43 d in 1994 (Kato & Kunjaya 1995). As presented orally in the conference held in Abano Terme, Italy, 1994 June 20–24, Robertson's team originally considered that the recurring NL-type bright state and the dwarf nova-type state in ER UMa and RZ LMi were the best examples to show the consequences of recurring mass-transfer bursts from the secondary. In the same conference, however, after Robertson's presentation, Y. Osaki introduced Kato and Kunjaya's detection of superhumps in ER UMa (Osaki 1995c) and showed that the unusual behavior of ER UMa could be understood within the framework of the thermal-tidal instability (TTI) model (Osaki 1989) if one can allow an exceptionally high mass-transfer rate (cf. Osaki 1995a). After this conference, Robertson's team published a paper following the interpretation by Kato and Kunjaya introduced by Y. Osaki (Robertson et al. 1994, 1995).[1] After the discovery of superhumps in ER UMa and the recognition of the similarity between ER UMa and RZ LMi, superhumps were naturally sought. The competition was intense: both Robertson, Honeycutt, and Turner (1995) and Nogami et al. (1995) observed the same superoutburst in 1995 and detected superhumps. These observations confirmed that RZ LMi does indeed belong to the SU UMa-type DNe. These objects, together with V1159 Ori, are usually called ER UMa-type stars (cf. Kato et al. 1999).

The mechanism of the ultrashort (19 d) supercycle and the unusually regular outburst pattern remained a mystery. Robertson, Honeycutt, and Turner (1994) suspected a mechanism outside the disk in addition to the one in the

[1] The dwarf nova-type nature was first clarified by Iida (1994). Misselt and Shafter (1995) also observed ER UMa in 1993–1994 and finally reached the same conclusion as Kato and Kunjaya (1995).

disk. A later publication by Olech et al. (2008) followed the former possibility and suggested a third body. In the standard TTI model, this short supercycle is difficult to reproduce, and Osaki (1995b) presented a working hypothesis that in RZ LMi the disk becomes thermally unstable during the superoutburst earlier than in other SU UMa-type DNe. Hellier (2001) suggested, following the interpretation in Osaki (1995b), that in systems with very small mass ratios (q), the tidal torque is too small to maintain the superoutburst, and that there occurs a decoupling between the thermal and tidal instabilities. Hellier (2001) suggested that one of the consequences of this decoupling can be found as the persistent superhumps after superoutbursts.

According to the working hypotheses by Osaki (1995b) and Hellier (2001), it is strongly predicted that the q is small in RZ LMi and that the disk radius after the superoutburst is larger than in other SU UMa-type DNe. RZ LMi, however, has defied every attempt to determine the orbital period, since it mostly stays in the "outburst" state and it is difficult to make a radial-velocity study in short quiescence. The almost continuous presence of superhumps also made it difficult to detect potential orbital variations by photometric methods. Without the orbital period or a radial-velocity study, it remained impossible to observationally determine q, and the evolutionary status of RZ LMi remained unclear despite its unusual outburst properties.

The situation dramatically changed after the detection of a possible change in the outburst pattern in the AAVSO observations (vsnet-alert 19524). We have conducted a world-wide campaign to observe RZ LMi during the 2016 season. The new development has also been helped by the classification of superhumps stage (A, B, and C: Kato et al. 2009) and identification of stage A superhumps representing the growing phase of superhumps at the radius of the 3 : 1 resonance (Osaki & Kato 2013b; Kato & Osaki 2013).

In this paper, key information and results are given in the main paper. The results not directly related to the conclusion of the paper, such as the variation of superhump periods and variation of the profile of superhumps, are given in the Supplementary Information, as they will provide useful information to expert readers.

2 Observations

The data were obtained under campaigns led by the VSNET Collaboration (Kato et al. 2004) in 2016. We also used the public data from the AAVSO International Database.[2] Time-resolved photometric observations were obtained on 75 nights (nights with more than 100 observations) between February 25 and June 10. Some snapshot observations were obtained on some other nights. We also performed time-resolved photometric observations during the period of 2013 March 5–April 29 at nine sites. We also obtained snapshot observations (several observations typically ~20 min apart) on 47 nights between 2014 March 8 and May 22. The logs of observations are given in the e-tables.[3] Alphabetical abbreviated codes in the log are observer codes of AAVSO and they mean that the data were taken from the AAVSO database. We also used historical photographic data reported by Pikalova and Shugarov (1995) (listed as "Shugarov," as he finally compiled all the data, in this paper).

The data were analyzed in the same way as described in Kato et al. (2009) and Kato et al. (2014b). We mainly used R software[4] for data analysis. In de-trending the data, we divided the data into four segments in relation to the outburst phase and used locally-weighted polynomial regression (LOWESS: Cleveland 1979). The times of superhumps maxima were determined by the template-fitting method as described in Kato et al. (2009). The times of all observations are expressed in barycentric Julian Days (BJD).

3 Results and discussion

3.1 Outburst light-curve and emergence of superhumps

Figure 1 illustrates the three consecutive superoutbursts in 2016 during which we obtained time-resolved photometric observations. The initial part of the light curve (upper panel) was the final fading part of the preceding superoutburst. There was only one normal outburst between the first and second superoutbursts. Although the initial part of the first superoutburst was not well sampled, we found that the superoutburst lasted for 26 d.

There were two normal outbursts between the second and the third superoutburst. The duration of the second superoutburst was 48 d, even longer than the first one. The intervals (supercycles) between the three superoutbursts were 32 d and 60 d. These values were 2–3 times longer than the historical supercycle (19 d) of this object (Robertson et al. 1994; Nogami et al. 1995).

During the best-observed second superoutburst, there was a shoulder (precursor outburst). Figure 2 shows the initial part of this superoutburst. The precursor part is clearly seen between BJD 2457483 and 2457484. During this phase, superhumps rapidly grew to the maximum amplitude and they started to decay slowly (lower panel; see

[2] ⟨http://www.aavso.org/data-download⟩.

[3] E-tables are available in the online edition as Supporting Information.

[4] The R Foundation for Statistical Computing ⟨http://cran.r-project.org/⟩.

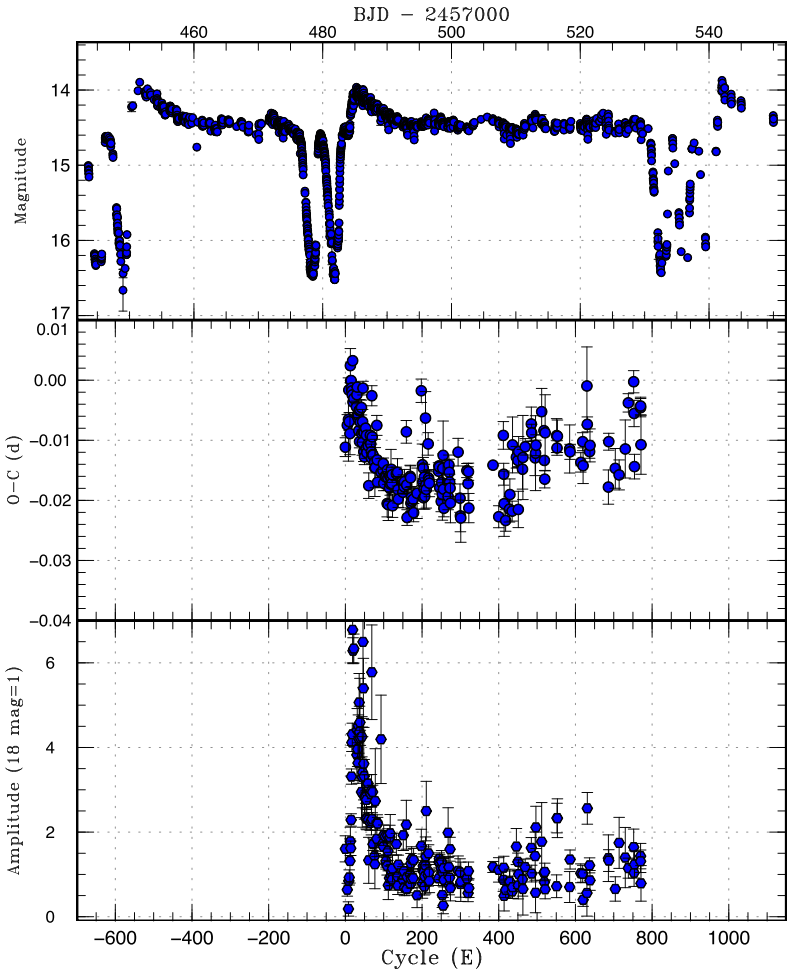

Fig. 1. Light-curve and $O-C$ diagram of superhumps in RZ LMi (2016). Upper: Light curve. The data were binned to 0.0023 d. In this figure, we show three consecutive superoutbursts which we observed. Middle: $O-C$ diagram for the second superoutburst (filled circles). We used a period of 0.05955 d for calculating the $O-C$ residuals. Lower: Amplitudes of superhumps. The scale is linear and the pulsed flux is shown in a unit corresponding to 18 mag = 1. (Color online)

also figure 3 for an enlargement). This behavior is the same as in ordinary SU UMa-type DNe [see e.g., figure 19 in Kato et al. (2013a) for one of the best-known SU UMa-type DNe VW Hyi; see also figure 4 in Osaki and Kato (2013a) for the corresponding part of the Kepler data of V1504 Cyg]. Similar precursors were also recorded in snapshot observations of the first superoutburst and less markedly (fewer observations) during the third superoutburst. These observations indicate that RZ LMi shows a sequence of a precursor and the main superoutburst as in ordinary SU UMa-type DNe at least in this season.

The variable supercycles now safely exclude the existence of a stable clock (such as an orbiting third body) which was supposed to work to produce regular superoutbursts (Robertson et al. 1994; Olech et al. 2008). Furthermore, Osaki (1995a) already showed that the supercycle length reaches the minimum as the mass-transfer rate ($\dot{M}$) increases, but that it lengthens again as $\dot{M}$ further increases. As $\dot{M}$ increases, the system eventually reaches the "permanent outburst" state (see figure 2 in Osaki 1995a), bridging ER UMa-type objects and what is called permanent superhumpers (Skillman & Patterson 1993; Patterson 1999). The current state of RZ LMi reproduced this prediction exactly, providing strong support to the explanation of the unusual short supercycles in ER UMa-type objects.

Osaki (1995b) formulated the duration of a superoutburst ($t_{\rm supermax}$) as below:

$$t_{\rm supermax} \sim t_{\rm vis}[f_M/(1-1/e)][1-(\dot{M}/\dot{M}_{\rm crit})]^{-1/2}, \quad (1)$$

where $t_{\rm vis}$ is the viscous depletion timescale and $\dot{M}_{\rm crit}$ is the critical $\dot{M}$ required to produce a hot, stable disk, respectively. The factor f_M is the fraction of the disk mass accreted during a superoutburst. It is given by

$$f_M \simeq 1-(R_0/R_{\rm d,crit})^{3.0}, \quad (2)$$

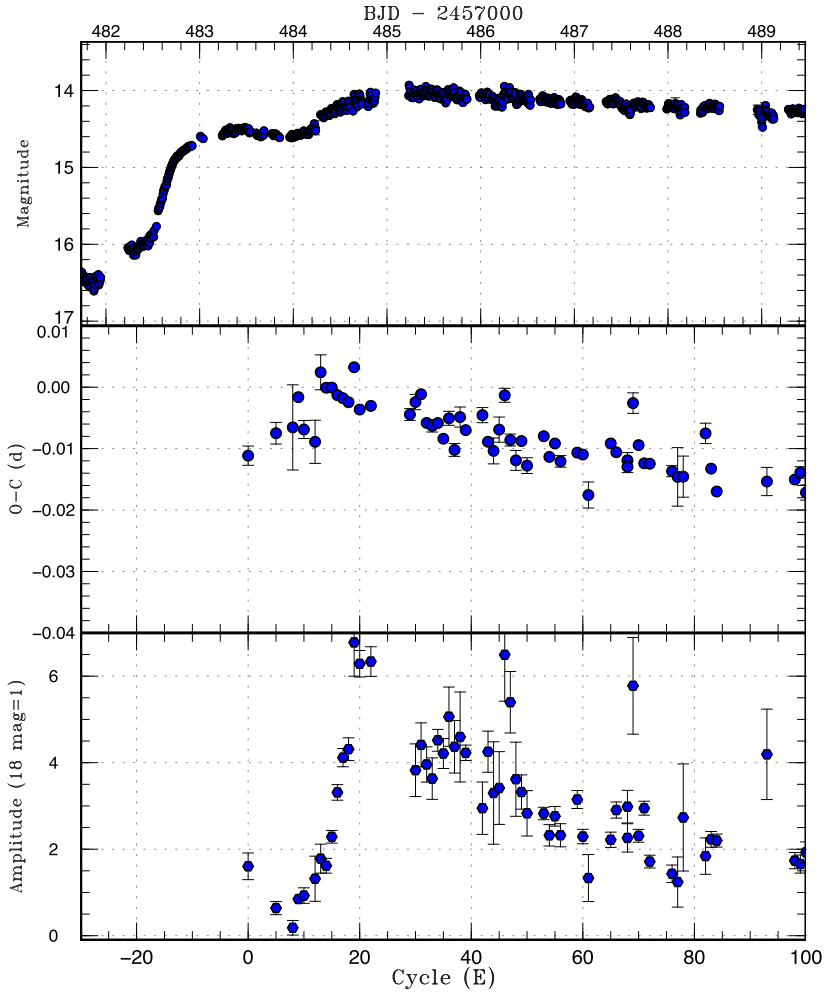

Fig. 2. Light-curve and $O-C$ diagram of superhumps in RZ LMi (2016). This figure is an enlargement of figure 1. Upper: Light curve. The data were binned to 0.0023 d. The precursor part is clearly seen between BJD 2457483 and 2457484. During this phase, superhumps rapidly grew. Middle: $O-C$ diagram for the second superoutburst (filled circles). We used a period of 0.05955 d for calculating the $O-C$ residuals. Lower: Amplitudes of superhumps. The scale is linear and the pulsed flux is shown in a unit corresponding to 18 mag = 1. (Color online)

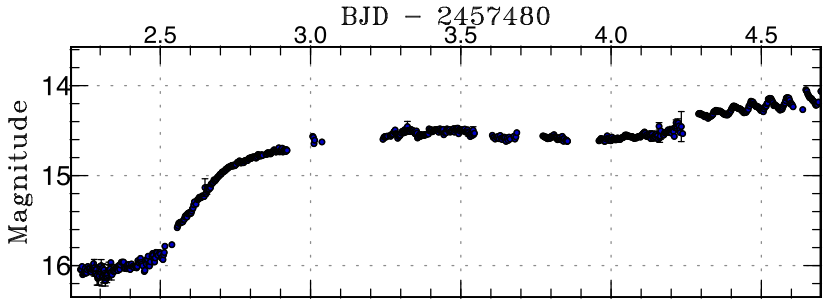

Fig. 3. Growing superhumps and precursor at the start of the 2016 April superoutburst. The data were binned to 0.0023 d. Superhump grew between BJD 2457483 and 2457484. (Color online)

where R_0 and $R_{\mathrm{d,\,crit}}$ represent the disk radius at the end of a superoutburst and at the start of a superoutburst (assuming that the disk critically reaches the radius of the 3 : 1 resonance at the start of a superoutburst), respectively. If we consider that t_{vis} and R_0 are the same between different superoutbursts of RZ LMi, we can estimate $\dot{M}$ during the current state. Using the parameters in Osaki (1995b), $t_{\mathrm{vis}} = 11.2$ d and an assumption of a large disk radius at the end of a superoutburst $R_0 = 0.42a$, where a is the binary separation, the historical t_{supermax} of 6 d (Robertson et al. 1995) is reproduced with $\dot{M}/\dot{M}_{\mathrm{crit}} = 0.5$. The current t_{supermax} values of 26 and 48 d require

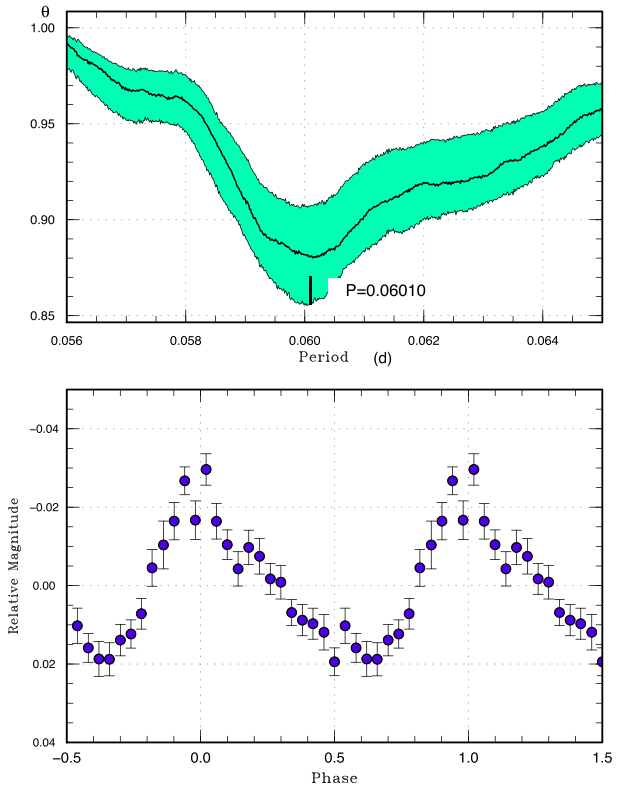

Fig. 4. Stage A superhumps in RZ LMi (2016). The data between BJD 2457483.01 and 2457484.40 were used. Upper: PDM analysis. We analyzed 100 samples which randomly contain 50% of observations, and performed PDM analysis for these samples. The bootstrap result is shown as a form of 90% confidence intervals in the resultant PDM θ statistics. Lower: Phase-averaged profile. (Color online)

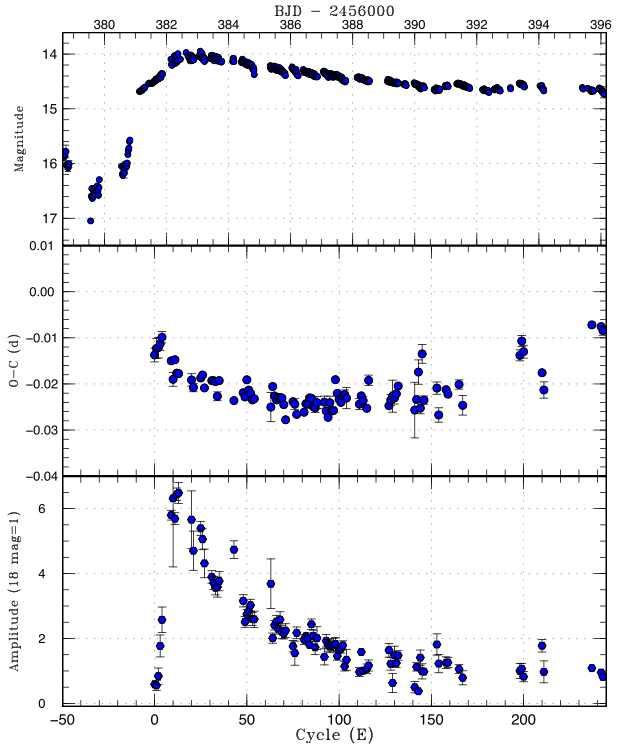

Fig. 5. $O-C$ diagram of superhumps in RZ LMi in 2013 April. Upper: Light curve. The data were binned to 0.0023 d. Middle: $O-C$ diagram (filled circles). We used a period of 0.05945 d for calculating the $O-C$ residuals. Lower: Amplitudes of superhumps. The scale is linear and the pulsed flux is shown in a unit corresponding to 18 mag = 1. (Color online)

$\dot{M}/\dot{M}_{\rm crit} = 0.97$ and 0.99, respectively. Although these estimates have uncertainties due to various assumptions, it is certain that the current state of RZ LMi is *critically* close to the stability border. If RZ LMi increases $\dot{M}$ further by 1%, the object should become a permanent superhumper. As judged from these estimates, we have seen an almost complete transition from an ER UMa-type object to a permanent superhumper. There has been at least one case (BK Lyn) in which a permanent superhumper became an ER UMa-type object and then returned back (Patterson et al. 2013; Kato et al. 2013a), and the case of RZ LMi may not be special.

3.2 Growing (stage A) superhumps and post-superoutburst superhumps

As is best seen in the lower panel of figure 2, the amplitudes of superhumps rapidly grew in ~20 cycles. During the initial ~13 cycles, the $O-C$ values (middle panel) were negative and a characteristic kink around $E = 13$ indicates that this object showed long-period (stage A) superhumps before entering the stable phase of stage B superhumps with a shorter period, as in other SU UMa-type DNe (see the e-tables for the full list of times of superhump maxima). This identification appears particularly confident since it has been recently demonstrated that ER UMa, the prototype of ER UMa-type objects, showed the same pattern with a precursor outburst (Ohshima et al. 2014). The period of stage A superhumps from the times of maxima ($E \leq 13$) is 0.0602(4) d. By using the data between BJD 2457483.01 and 2457484.40, we have obtained a period of 0.0601(1) d with the phase dispersion minimization (PDM: Stellingwerf 1978) method (figure 4). The errors are 1σ estimated by the methods of Fernie (1989) and Kato et al. (2010). We consider that the result by the PDM method is more reliable than that from superhump maxima, since it gives a smaller error, and adopted this period.

Although the second superoutburst was generally well observed, the observations were unfortunately relatively sparse around stage A. The 2013 April superoutburst of this object was relatively well observed in the same phase, although the brightness peak was missed and instead of a distinct precursor there was a stagnation in the rising phase, which was likely an embedded precursor (figures 5 and 6; see e-table for the full times of superhump maxima). During the observation in 2013, a continuous light curve

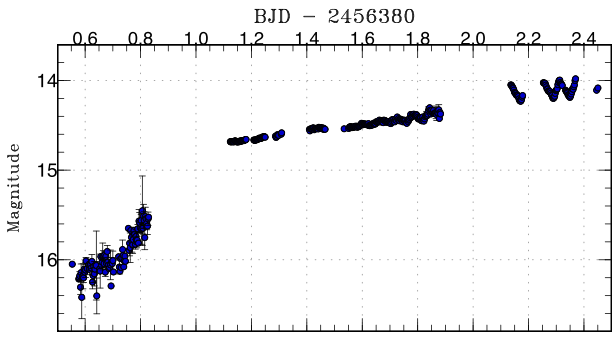

Fig. 6. Growing superhumps and stagnation (embedded precursor) at the start of the 2013 April superoutburst. The data were binned to 0.0023 d. Superhump grew between BJD 2456381.41 and 2456381.88. (Color online)

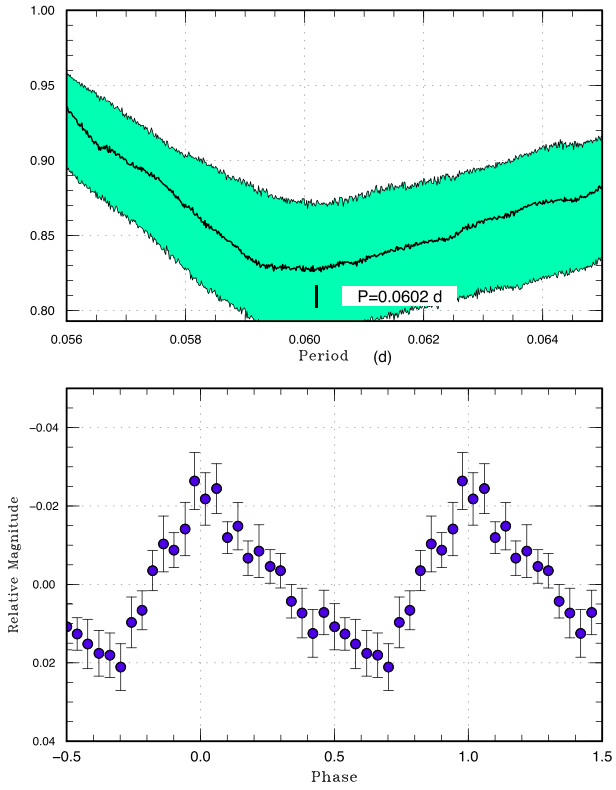

Fig. 7. Stage A superhumps in RZ LMi (2013 April). The data between BJD 2456381.41 and 2456381.88 were used. Upper: PDM analysis. Lower: phase-averaged profile. (Color online)

of growing superhumps ($0 \leq E \leq 4$) was well recorded. Using the data between BJD 2456381.41 and 2456381.88, we obtained a period of 0.0602(3) d with the PDM method (figure 7). Since this value is consistent with the 2016 one, we adopted an averaged value of 0.0602(1) d as the period of stage A superhumps.

The dynamical precession rate, $\omega_{\rm dyn}$, in the disk can be expressed by (see Hirose & Osaki 1990):

$$\omega_{\rm dyn}/\omega_{\rm orb} = Q(q)R(r), \tag{3}$$

where $\omega_{\rm orb}$ and r are the angular orbital frequency and the dimensionless radius measured in units of the binary separation a. The dependencies on q and r are

$$Q(q) = \frac{1}{2}\frac{q}{\sqrt{1+q}}, \tag{4}$$

and[5]

$$R(r) = \frac{1}{2}\sqrt{r}b^{(1)}_{3/2}(r), \tag{5}$$

where $\frac{1}{2}b^{(j)}_{s/2}$ is the Laplace coefficient;

$$\frac{1}{2}b^{(j)}_{s/2}(r) = \frac{1}{2\pi}\int_0^{2\pi}\frac{\cos(j\phi)d\phi}{(1+r^2-2r\cos\phi)^{s/2}}. \tag{6}$$

This $\omega_{\rm dyn}/\omega_{\rm orb}$ is equal to the fractional superhump excess in frequency: $\epsilon^* \equiv 1 - P_{\rm orb}/P_{\rm SH}$, where $P_{\rm orb}$ and $P_{\rm SH}$ are the orbital period and superhump period, respectively. If $P_{\rm orb}$ is known, we can directly determine q from the observed ϵ^* of stage A superhumps under the assumption that the period of stage A superhumps reflects the purely dynamical precession rate at the radius of the 3 : 1 resonance (Kato & Osaki 2013).

Since the orbital period of RZ LMi is not known, we cannot directly apply the method in Kato and Osaki (2013) to determine q dynamically. We can instead use the period of post-superoutburst superhumps to constrain q and the disk radius as introduced in Kato et al. (2013b):

$$\epsilon^*({\rm stageA}) = Q(q)R(r_{3:1}) \tag{7}$$

and

$$\epsilon^*({\rm post}) = Q(q)R(r_{\rm post}), \tag{8}$$

where $r_{3:1}$ is the radius of the 3 : 1 resonance;

$$r_{3:1} = 3^{(-2/3)}(1+q)^{-1/3}, \tag{9}$$

ϵ^*(post) and $r_{\rm post}$ are the fractional superhump excess and disk radius immediately after the outburst, respectively. By solving equations (7) and (8) simultaneously, we can obtain the relation between $r_{\rm post}$ and q. If we have knowledge about $r_{\rm post}$, as determined in other systems in Kato and Osaki (2013), we have a more stringent constraint.

On 2013 March 20, the object was observed in quiescence closely following a superoutburst which started on

[5] There was a typographical error in the second line of equation (1) in Kato and Osaki (2013). The correct formula is $\frac{q}{\sqrt{1+q}}\left[\frac{1}{4}\sqrt{r}b^{(1)}_{3/2}\right]$. The results (including tables) in Kato and Osaki (2013) used the correct formula and the conclusions are unchanged. We used the correct formula in equation (5) in this paper. The same correction of the equation should be applied to Kato et al. (2013b), Nakata et al. (2013), and Kato (2015).

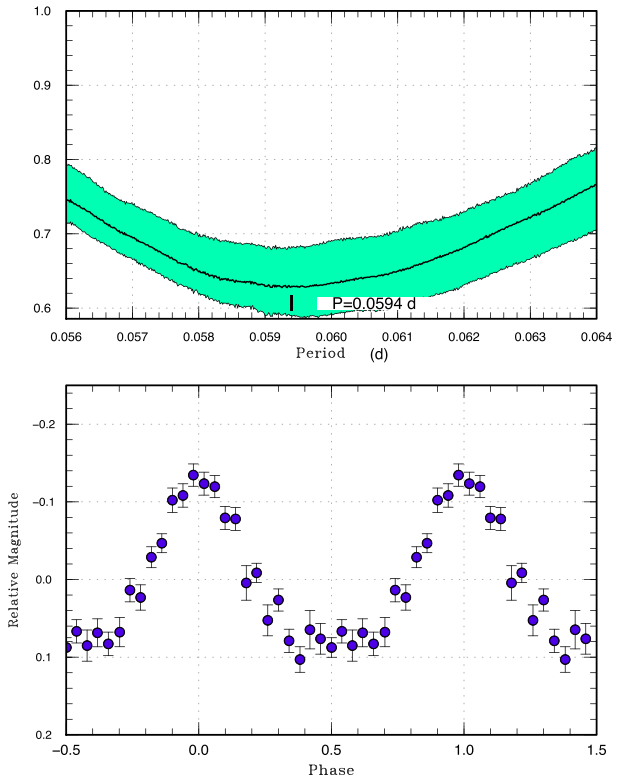

Fig. 8. Post-superoutburst superhumps in RZ LMi (2013 March 20). The data between BJD 2456371.5 and 2456371.9 were used. Upper: PDM analysis. Lower: Phase-averaged profile. (Color online)

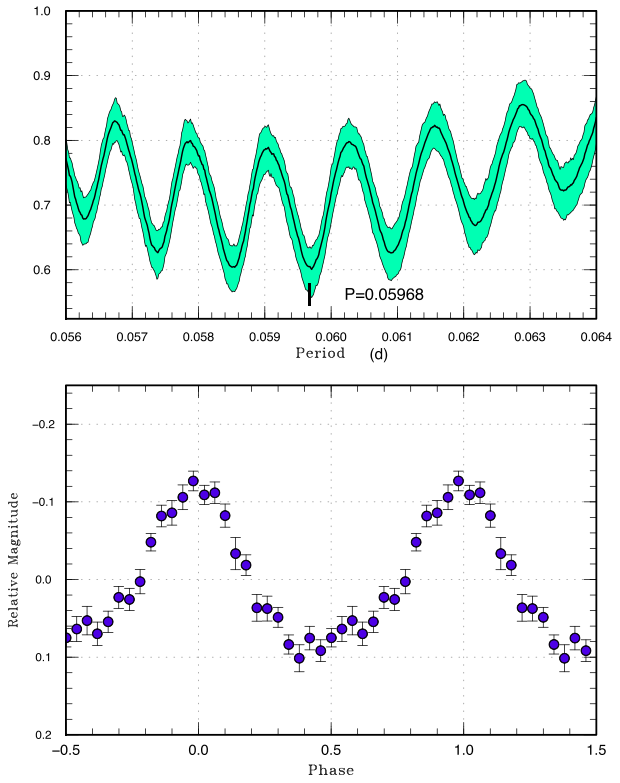

Fig. 9. Post-superoutburst superhumps in RZ LMi (2013 March 20 and 24). Upper: PDM analysis. Lower: Phase-averaged profile. (Color online)

March 6. The object displayed post-superoutburst superhumps and there was a continuous run covering six cycles. A PDM analysis of this continuous run yielded a period of 0.0594(2) d (figure 8). Since this variation was also present after one further normal outburst, and since the decaying amplitudes of this variation exclude the possibility of the orbital variation, we identified this period as that of post-superoutburst superhumps. We combined the quiescent data on March 20 and 24 and obtained a period of 0.05969(2) d (figure 9, assuming that the superhump phase and period did not change during a normal outburst). The shorter one-day alias (∼0.0584 d) is too close to the supposed orbital period (discussed later) and this alias is unlikely.

Using the periods of stage A superhumps and post-superoutburst superhumps, the relation between $r_{\rm post}$ and q is shown in figure 10. The measurements of $r_{\rm post}$ in SU UMa-type DNe using the same method are within the range of 0.30 and 0.38 (Kato & Osaki 2013). The smaller values represent the values for WZ Sge-type DNewith multiple rebrightenings (after such rebrightenings), and it is extremely unlikely to be the case for RZ LMi. If $r_{\rm post}$ is around 0.38, q is estimated to be 0.06(1). It would be noteworthy that Osaki (1995b) assumed $r_{\rm post} = 0.42$ for this particular object. If this is indeed the case, q needs to be as large as 0.10(2). This consideration suggests that the expectations of Osaki (1995b) and Hellier (2001) that RZ LMi has a very small q and that the large disk radius immediately following a superoutburst are not true at the same time: either q is higher or the disk radius is smaller. This is the important conclusion from the present observation. Since stage A superhumps were not very ideally observed in the present study, further observations are needed to refine the result.

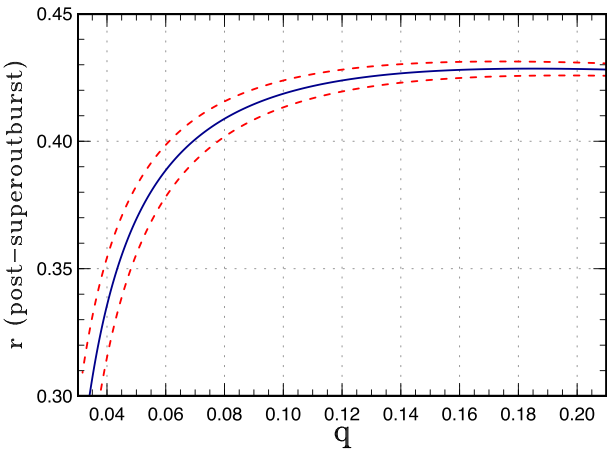

Fig. 10. Relation between q and $r_{\rm post}$ using the periods of stage A superhumps and post-superoutburst superhumps. Dashed curves represent the range of 1σ errors. (Color online)

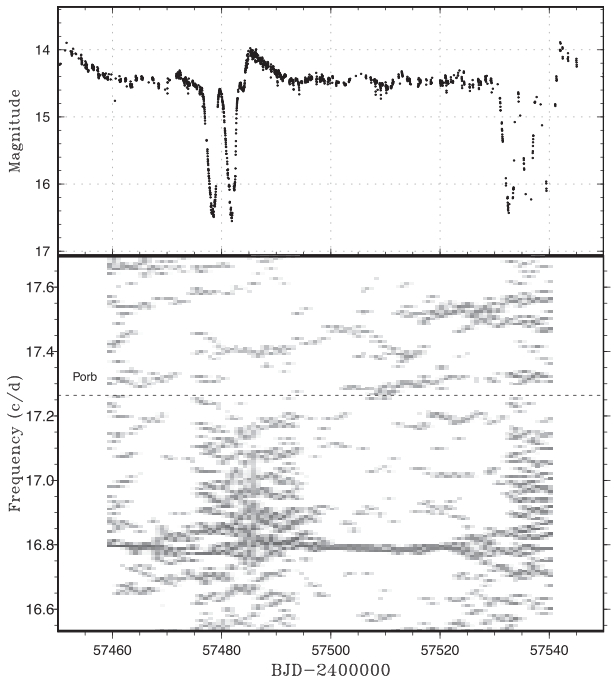

Fig. 11. Two-dimensional Lasso period analysis of RZ LMi (2016). Upper: Light curve. The data were binned to 0.02 d. Lower: Lasso period analysis. The strong persistent signal (disturbed during the starting phase of the superoutburst due to the non-sinusoidal profile and rapidly varying periods) around 16.8 c d^{-1} is superhumps. A weaker signal around 17.50–17.55 c d^{-1} between BJD 2457510 and 2457530 is possible negative superhumps. $\log\lambda = -6.4$ was used. Porb represents the orbital period we suggest. The widths of the sliding window and the time step used are 18 d and 0.8 d, respectively.

3.3 Possible negative superhumps and orbital period

We used the least absolute shrinkage and selection operator (Lasso) method (Tibshirani 1996; Kato & Uemura 2012), which has been proven to yield very sharp signals. We used the two-dimensional Lasso power spectra as introduced in the analysis of the Kepler data in such studies as Kato and Maehara (2013) and Osaki and Kato (2013b). These two-dimensional Lasso power spectra have been proven to be very effective in detecting signals in non-uniformly sampled ground-based data (see e.g., Ohshima et al. 2014) since Lasso-type period analysis is less affected by aliasing than traditional Fourier-type power spectra. This characteristic has enabled detection of negative superhumps in ground-based observations (e.g., Ohshima et al. 2014; Kato et al. 2014b). The result for RZ LMi in 2016 is shown in figure 11. The strong persistent signal around 16.8 cycles per day (c d^{-1}) is superhumps. A weaker signal around 17.50–17.55 c d^{-1} between BJD 2457510 and 2457530 is possible negative superhumps. Since the second superoutburst lasted for a very long time, it may have been possible that negative superhumps were excited during this long-lasting standstill-like phase, which gives a condition that is almost the same as that in permanent superhumpers (see subsection 3.1). A PDM analysis of the data between BJD 2457510 and 2457530 yielded a period of 0.05710(1) d. The superhump period in this interval was 0.059555(4) d.

It has been widely accepted that absolute fractional superhumps excesses (ϵ_+ for positive superhumps, and ϵ_- for negative superhumps, where $\epsilon \equiv P_{\rm SH}/P_{\rm orb} - 1$) are tightly correlated when both signals are simultaneously seen in NL CVs (e.g., Patterson et al. 1997; Montgomery 2009). The empirical relation is $\epsilon_+ \simeq 2|\epsilon_-|$. If it is also the case for RZ LMi, $P_{\rm orb}$ is expected to be around 0.05792 d. This period is labeled as Porb in figure 11. If this is indeed the orbital period, the consequence is important (cf. subsection 3.2). The measured period of stage A superhumps [0.0602(1) d] gives $\epsilon^* = 0.038(2)$, which is equivalent to $q = 0.105(5)$ [see table 1 in Kato and Osaki (2013). This value is higher than the typical ones for WZ Sge-type DNe, which have similar $P_{\rm orb}$ as RZ LMi (Kato & Osaki 2013; Kato 2015; Kato et al. 2016b). This q measurement invalidates the suggestion by Osaki (1995b) and Hellier (2001) that the unusual properties of RZ LMi is a result of the very low q. The q, however, is consistent with the relation derived from the period of stage A and post-superoutburst superhumps (subsection 3.2, figure 10) assuming the large disk radius at the end of a superoutburst. If this interpretation is correct, the disk radius at the end of a superoutburst is large, as required by Osaki (1995b), but the origin of the large disk (i.e., superoutbursts which terminate earlier than in ordinary SU UMa-type DNe) cannot be attributed to an exceptionally small q. In recent years, some SU UMa-type DNe show early termination of superoutbursts (such as V1006 Cyg, Kato et al. 2016a). In Kato et al. (2016a), the termination may be associated with the supposed appearance of stage C superhumps (late-stage superhumps with a shorter constant period). The origin of stage C superhumps is still poorly known, and the reason for the premature termination of superoutbursts, which may be related to the evolution of stage C superhumps, still needs to be clarified.

There is supporting evidence for a large q: the duration of stage A superhumps, which is considered to reflect the growth time of the 3 : 1 resonance, is very short (less than 1 d) in RZ LMi. From a theoretical standpoint, this growth time is expected to be proportional to $1/q^2$ (Lubow 1991), and this relation has been confirmed in WZ Sge-type DNe(Kato 2015). As judged from the rapid growth of superhumps in RZ LMi, it appears extremely unlikely that RZ LMi has as small a q as in WZ Sge-type DNe.

3.4 Evolutionary status

If the q derived from the possible negative superhumps and suggested by the rapid growth of superhumps (subsection 3.3) is correct, RZ LMi cannot be an object

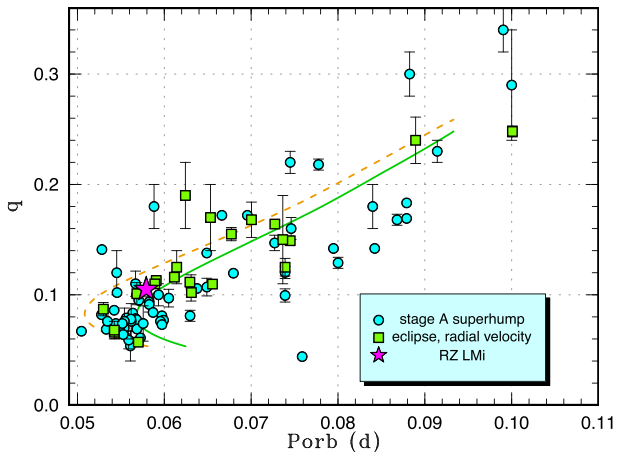

Fig. 12. Location of RZ LMi on the diagram of mass ratio versus orbital period. The dashed and solid curves represent the standard and optimal evolutionary tracks in Knigge, Baraffe, and Patterson (2011), respectively. The filled circles, filled squares, filled stars, and filled diamonds represent q values from a combination of the estimates from stage A superhumps published in six preceding sources (Kato & Osaki 2013; Nakata et al. 2013; Kato et al. 2014a, 2014b, 2015, 2016b), known q values from quiescent eclipses or radial-velocity study (see Kato & Osaki 2013 for the data source). In addition to the references listed in Kato et al. (2016b), we supplied the data for SDSS J143317.78+101123.3 in Hernández Santisteban et al. (2016). (Color online)

close to the period minimum or a period bouncer—Olech et al. (2008) conjectured that some ER UMa-type novae are period bouncers. The q we suggested is similar to or even larger than those of ordinary SU UMa-type DNe having similar $P_{\rm orb}$ (figure 12).

We know of at least one other object, GALEX J194419.33+491257.0 in the Kepler field, which has a very short $P_{\rm orb}$ of 0.0528164(4) d and very frequent outbursts (normal outbursts with intervals of 4–10 d) (Kato & Osaki 2014). This object has an unusually high q = 0.141(2) measured using stage A superhumps. These properties are somewhat similar to those of RZ LMi. Kato and Osaki (2014) suggested the possibility that GALEX J194419.33+491257.0 may be a CV with a stripped core-evolved secondary and which is evolving toward an AM CVn-type CV. Such a condition might be a fascinating possibility to explain why RZ LMi has an exceptionally high $\dot{M}$ for its $P_{\rm orb}$.

3.5 Secular variation of supercycle

As discussed in subsection 3.1, it is likely that RZ LMi changed $\dot{M}$ by a factor of $\sim$2 in the last two decades. In recent years, a transition from the NL (permanent superhumper) state to the ER UMa-type state was discovered in BK Lyn (Patterson et al. 2013; Kato et al. 2013a). Patterson et al. (2013) proposed, based on the potential identification with an ancient classical nova in 101, that ER UMa stars are transitional objects during the cooling phase of post-eruption classical novae [the idea was not new and it was already proposed in Kato and Kunjaya (1995) and Osaki (1995a)]. Following this interpretation, Otulakowska-Hypka and Olech (2013) studied ER UMa-type objects and found a secular increase of the supercycle in most typical ER UMa-type objects. RZ LMi was included, and Otulakowska-Hypka and Olech (2013) gave a $\dot{P}$ of the supercycle of $(5.0 \pm 1.9) \times 10^{-4}$ in 18 yr. We should note that Zemko, Kato, and Shugarov (2013) also studied variation of supercycles in ER UMa and reported that supercycles vary in a range of 43.6–59.2 d with shorter time-scales of 300–1900 d. A secular increase of the supercycle was also statistically meaningful in that work (Zemko et al. 2013).

The conclusion of Otulakowska-Hypka and Olech (2013), however, was only based on the variation of supercycles, and they disregarded the possibility that the supercycle can also increase if $\dot{M}$ increases toward $\dot{M}_{\rm crit}$ since there is a minimum in the supercycle as $\dot{M}$ increases [cf. the right-hand branch of figure 1 in Osaki (1995a); see also subsection 3.1]. As this is apparently the case for RZ LMi, we studied the secular variation of supercycles in RZ LMi. We summarize the result in table 1 [the data in Kato et al. (2013a) also used AAVSO observations]. When raw data were not available, we measured the fraction of superoutburst and duty cycle by eye from the figures in the papers listed in the table. The data for 1986–1989 (Shugarov) were too sparse to determine the supercycle and only the duty cycle was estimated. The data for 1987–1988 (Kato) were visual observations. The supercycle was determined from seven well-defined bright outbursts. The duty cycle was probably underestimated due to the insufficient detection limit of visual observations. For AAVSO observations, the fraction of superoutbursts could be determined only to 0.05 since most of the data were randomly sampled snapshot observations.

It has became apparent that the supercycle was not stable as had been supposed in Robertson, Honeycutt, and Turner (1995) and Olech et al. (2008). The supercycle at the time of Robertson, Honeycutt, and Turner (1995) probably reached the historical minimum. It was likely the supercycle once lengthened to as much as $\sim$24 d before 2013, but it returned to 19–20 d. This behavior probably gave the impression that the supercycle is globally constant if seen in long time-scales, such as several years. The situation changed in 2016 when the supercycle strongly increased. This increase was associated with the increase of the fraction of superoutburst and the duty cycle, indicating that $\dot{M}$ increased despite the lengthening of the supercycle [contrary to the conclusion by Otulakowska-Hypka and Olech (2013)]. Although the situation before 2016 was less clear,

Table 1. Supercycles of RZ LMi.

Year	JD range*	Supercycle (d)	Fraction of superoutburst	Duty cycle†	Nights	Source
1984	45699–45851	19.6(1)	0.4	0.53	30	This work (Shugarov)
1984–1985	46019–46230	19.5–21.5	0.35:	0.39	31	This work (Shugarov)
1986–1989	46468–47682	—	—	0.6	7	This work (Shugarov)
1987–1988	47151–47318	22.5(9)	—	0.39	52	This work (Kato)
1992–1995	48896–49723	18.87	0.4	0.5	—	Robertson, Honeycutt, and Turner (1995)
2004–2005	53027–53519	19.07(4)	0.4	0.4	—	Olech et al. (2008)
2005–2006	53644–53884	19.7(1)	0.45	0.58	89	AAVSO
2006–2007	54041–54254	20.75(4)	0.40	0.55	113	AAVSO
2007–2008	54374–54626	21.3(1)	0.45	0.55	100	AAVSO
2008–2009	54749–54988	21.7(1)	0.40	0.31	96	AAVSO
2009–2010	55146–55334	24.3(1)	0.35	0.52	58	AAVSO
2012	55985–56070	21.61(2)	0.55	0.46	76	Kato et al. (2013a)
2012–2013	56273–56473	22.83(1)	0.50	0.62	149	This work
2013–2014	56563–56819	20.8(1)	0.40	0.48	151	This work (Neustroev), AAVSO
2014–2015	56930–57178	19.9(1)	0.45	0.55	96	AAVSO
2016	57416–57451	35	0.60	0.50	28	This work
2016	57451–57483	32	0.81	0.74	31	This work
2016	57483–57543	60	0.80	0.83	54	This work

*JD−2400000.
†Object brighter than 15.0 mag.

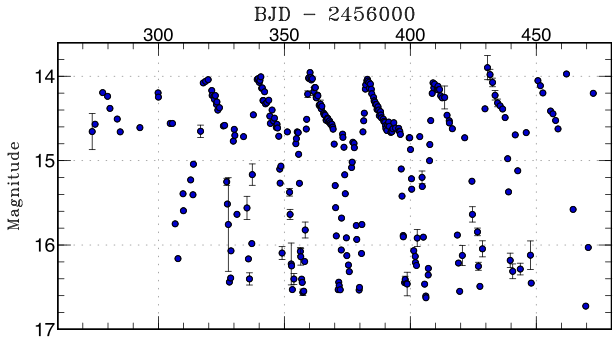

Fig. 13. Overall light-curve of RZ LMi in 2013. The data were binned to 0.03 d. (Color online)

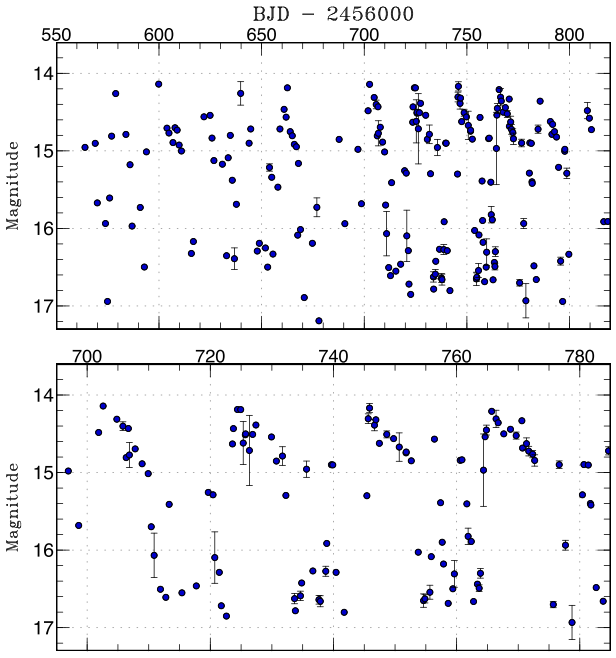

Fig. 14. Overall light-curve of RZ LMi in 2013–2014. The data were binned to 0.03 d. (Color online)

the changing supercycle suggests fluctuating $\dot{M}$ within time scales of a year or two. The outburst pattern was generally regular in the second best-observed season in 2013 (figure 13). The duration of the superoutburst was appreciably longer between BJD 2456380 and 2456400 (17 d, in contrast to 12–13 d in other superoutbursts in 2013; a mean value of supercycles in 2013 is given in table 1). It was likely that $\dot{M}$ temporarily increased also in 2013. In the 2013–2014 season, the durations of superoutbursts again decreased to shorter than 12 d (figure 14) while supercycle lengths remained short (∼21 d).

As far as RZ LMi is concerned, $\dot{M}$ is not secularly decreasing as in the scenario given by Patterson et al. (2013). Among other ER UMa-type objects, BK Lyn returned to its original NL state in late 2013 and the ER UMa-type state was only transiently present (Kato et al. 2013a). As discussed in Kato et al. (2013a), the hypothetical cooling sequence from NL objects → ER UMa-type DNe → ordinary SU UMa-type DNe after nova eruptions as proposed

by Patterson et al. (2013) is not very consistent with observational statistics, since such a cooling sequence would predict a large number of intermediate (having much more slowly cooling white dwarfs) objects between ER UMa-type DNeand ordinary SU UMa-type DNe, while observations could not confirm a large number of such objects. As seen in ER UMa, BK Lyn, and RZ LMi, the $\dot{M}$ variations look more irregular with time-scales of several years and it looks like that the majority of variations in outburst activities in these systems does not reflect the secular $\dot{M}$ variation as proposed by Patterson et al. (2013). As this paper has shown, the high activity of RZ LMi may be a result of a rare evolutionary condition with a relatively massive secondary. In such a case, we may not require a nova eruption to produce an object like RZ LMi.

4 Summary

We observed RZ LMi, which is renowned for the extremely (∼19 d) short supercycle and is a member of a small, unusual class of CV called ER UMa-type DNe, in 2013 and 2016. In 2016, the supercycles of this object substantially lengthened in comparison to the previous measurements to 35, 32, and 60 d for three consecutive superoutbursts. The durations of the superoutbursts also lengthened and they composed 60%–81% of the supercycle. Such long durations of superoutbursts have never been observed in this object, and we consider that the object virtually experienced a transition to the NL state (permanent superhumper). This observed behavior reproduced the prediction of the thermal-tidal instability model made by Osaki (1995a) extremely well. We estimated that in 2016, the mass-transfer rate of RZ LMi reached 97%–99% of the thermal stability limit, and that it was about two times larger than the value in the past.

We detected a precursor in the 2016 superoutburst and detected growing (stage A) superhumps in 2016 and in 2013. We estimated their period to be 0.0602(1) d. This makes the second case in which growing superhumps were confidently recorded in ER UMa-type DNe during the sequence of the precursor and the main superoutburst. We also detected post-superoutburst superhumps immediately after a superoutburst in 2013 with a period of 0.05969(2) d. Since both stage A superhumps and post-superoutburst superhumps can be considered to reflect the dynamical precession rates, we can derive the relation between the mass ratio and the radius of the post-superoutburst. The result suggests that the mass ratio is not as small as in WZ Sge-type DNe, having orbital periods similar to RZ LMi.

By using Lasso two-dimensional power spectra, we detected possible negative superhumps with a period of 0.05710(1) d. By combination with the period of ordinary superhumps, we estimated the orbital period of 0.05792 d. The period of stage A superhumps, combined with this orbital period, suggests a mass ratio of 0.105(5). This relatively large mass ratio is consistent with the rapid growth of superhumps. This mass ratio is even above ordinary SU UMa-type DNe, and it is also possible that the exceptionally high mass-transfer rate in RZ LMi may be a result of a stripped core evolved secondary in a system evolving toward an AM CVn-type object.

An analysis of historical records of supercycles in this system suggests that the variation of the outburst activity is sporadic with time-scales of years and it does not seem to reflect the secular variation caused by evolution.

Acknowledgement

This work was supported by the Grant-in-Aid "Initiative for High-Dimensional Data-Driven Science through Deepening of Sparse Modeling" (25120007) from the Ministry of Education, Culture, Sports, Science and Technology (MEXT) of Japan. CCN thanks the funding from National Science Council of Taiwan under the contract NSC101-2112-M-008-017-MY3. This work also was partially supported by RFBR grant 15-02-06178 (Crimean team, Shugarov and Katysheva) and Grant VEGA No. 2/0002/13 (Shugarov, Chochol, Sekeráš). This study was also supported by the Science Committee of the Science and Education Ministry of Kazakhstan (project No. 0075/GF4). The authors are grateful to observers of VSNET Collaboration and VSOLJ observers who supplied vital data. We acknowledge with thanks the variable star observations from the AAVSO International Database contributed by observers worldwide and used in this research. This research has made use of the SIMBAD database, operated at CDS, Strasbourg, France.

Supporting information

Supplementary data are available at *PASJAP* online.

E-tables 1–11 and e-figures 1–13.

References

Abrahamian, H. V., & Mickaelian, A. M. 1993, Astrofiz., 36, 109
Cleveland, W. S. 1979, J. Am. Statist. Assoc., 74, 829
Fernie, J. D. 1989, PASP, 101, 225
Green, R. F., Ferguson, D. H., Liebert, J., & Schmidt, M. 1982, PASP, 94, 560
Hellier, C. 2001, PASP, 113, 469
Hernández Santisteban, J. V., et al. 2016, Nature, 533, 366
Hirose, M., & Osaki, Y. 1990, PASJ, 42, 135
Iida, M. 1994, VSOLJ Variable Star Bull., 19, 2
Kato, T. 2015, PASJ, 67, 108
Kato, T., et al. 2009, PASJ, 61, S395
Kato, T., et al. 2010, PASJ, 62, 1525
Kato, T., et al. 2013a, PASJ, 65, 23
Kato, T., et al. 2014a, PASJ, 66, 30
Kato, T., et al. 2014b, PASJ, 66, 90

Kato, T., et al. 2015, PASJ, 67, 105
Kato, T., et al. 2016a, PASJ, 68, L4
Kato, T., et al. 2016b, PASJ, 68, 65
Kato, T., & Kunjaya, C. 1995, PASJ, 47, 163
Kato, T., & Maehara, H. 2013, PASJ, 65, 76
Kato, T., Monard, B., Hambsch, F.-J., Kiyota, S., & Maehara, H. 2013b, PASJ, 65, L11
Kato, T., Nogami, D., Baba, H., Masuda, S., Matsumoto, K., & Kunjaya, C. 1999, in Disk Instabilities in Close Binary Systems, ed. S. Mineshige & J. C. Wheeler (Tokyo: Universal Academy Press), 45
Kato, T., & Osaki, Y. 2013, PASJ, 65, 115
Kato, T., & Osaki, Y. 2014, PASJ, 66, L5
Kato, T., & Uemura, M. 2012, PASJ, 64, 122
Kato, T., Uemura, M., Ishioka, R., Nogami, D., Kunjaya, C., Baba, H., & Yamaoka, H. 2004, PASJ, 56, S1
Kholopov, P. N., Samus, N. N., Kazarovets, E. V., & Perova, N. B. 1985, IBVS, 2681
Knigge, C., Baraffe, I., & Patterson, J. 2011, ApJS, 194, 28
Kondo, M., Noguchi, T., & Maehara, H. 1984, Tokyo Astron. Obs. Ann., Sec. Ser., 20, 130
Lipovetskii, V. A., & Stepanyan, J. A. 1981, Astrofiz., 17, 573
Lubow, S. H. 1991, ApJ, 381, 259
Misselt, K. A., & Shafter, A. W. 1995, AJ, 109, 1757
Montgomery, M. M. 2009, ApJ, 705, 603
Nakata, C., et al. 2013, PASJ, 65, 117
Nogami, D., Kato, T., Masuda, S., Hirata, R., Matsumoto, K., Tanabe, K., & Yokoo, T. 1995, PASJ, 47, 897
Ohshima, T., et al. 2014, PASJ, 66, 67
Olech, A., Wisniewski, M., Zloczewski, K., Cook, L. M., Mularczyk, K., & Kedzierski, P. 2008, Acta Astron., 58, 131
Osaki, Y. 1989, PASJ, 41, 1005
Osaki, Y. 1995a, PASJ, 47, L11
Osaki, Y. 1995b, PASJ, 47, L25
Osaki, Y. 1995c, in Cataclysmic Variables, ed. A. Bianchini et al. (Dordrecht: Kluwer Academic Publishers), 307
Osaki, Y., & Kato, T. 2013a, PASJ, 65, 50
Osaki, Y., & Kato, T. 2013b, PASJ, 65, 95
Otulakowska-Hypka, M., & Olech, A. 2013, MNRAS, 433, 1338
Patterson, J. 1999, in Disk Instabilities in Close Binary Systems, ed. S. Mineshige & J. C. Wheeler (Tokyo: Universal Academy Press), 61
Patterson, J., Kemp, J., Saad, J., Skillman, D. R., Harvey, D., Fried, R., Thorstensen, J. R., & Ashley, R. 1997, PASP, 109, 468
Patterson, J., et al. 2013, MNRAS, 434, 1902
Pikalova, O. D., & Shugarov, S. Yu. 1995, in Cataclysmic Variables, ed. A. Bianchini et al. (Dordrecht: Kluwer Academic Publishers), 173
Robertson, J. W., Honeycutt, R. K., & Turner, G. W. 1994, in ASP Conf. Ser. 56, Interacting Binary Stars, ed. A. W. Shafter (San Francisco: ASP), 298
Robertson, J. W., Honeycutt, R. K., & Turner, G. W. 1995, PASP, 107, 443
Skillman, D. R., & Patterson, J. 1993, ApJ, 417, 298
Stellingwerf, R. F. 1978, ApJ, 224, 953
Tibshirani, R. 1996, J. R. Stat. Soc. Ser. B, 58, 267
Warner, B. 1995, Cataclysmic Variable Stars (Cambridge: Cambridge University Press)
Zemko, P., Kato, T., & Shugarov, S. 2013, PASJ, 65, 54